NGVLA Memo 101: Mapping the Gas Density and Kinematic Structures due to Embedded Protoplanets in Young Disks with the Next Generation Very Large Array

L. Ricci[1,*], B. Burrill[1], I. Rabago[2], Z. Zhu[2]

[1] *Department of Physics and Astronomy, California State University Northridge, 18111 Nordhoff Street, Northridge, CA 91330, USA*

[2] *Department of Physics and Astronomy, University of Nevada Las Vegas, Las Vagas, NV 89154, USA*

[*] *Corresponding author: Luca Ricci, luca.ricci@csun.edu*

Abstract. We present simulations of the capabilities of the Next Generation Very Large Array to detect and resolve substructures due to the interaction with planets in the ^{12}CO molecular gas emission of nearby planet-forming disks. Whereas previous ngVLA studies on the disk-planet interaction focused on the dust continuum emission, this study investigates the effects of a Jupiter-mass planet on the channel maps for the ^{12}CO ($J = 1 - 0$) emission line from the disk, which can be observed at ngVLA Band 6. For this investigation we adopt the results of global 3-D hydrodynamical planet-disk simulations that account for the dynamics of gas in a disk with an embedded planet. Our work shows that the ngVLA can detect and spatially resolve the density and kinematic signatures expected in the disk CO emission and due to Jupiter-mass planets at intermediate separations from the host star in nearby star forming regions.

1. Introduction

The discovery of thousands of exoplanets over the last couple of decades has shown that the birth of planets in young circumstellar disks made of gas and solids is a very efficient process in nature (see Andrews 2020, for a review).

Although planets are known to form in disks rotating around young stars, finding evidence of newly born planets is extremely difficult. The two main reasons that hamper the detection of young forming planets are (i) the presence of the circumstellar material which can easily absorb radiation from an embedded planet (e.g., Sanchis et al. 2020) and contaminate the light curve of the host star, and (ii) the intense activity of young stars which makes it difficult to discern planetary signatures from the stellar radial velocity and light curve. Because of this, finding indirect evidence for the presence of planets in the density and kinematics of matter in the disk is the most powerful viable method to characterize the population of the very young forming planets which are still deeply embedded in the disk (Zhang et al. 2018).

In fact, high-angular resolution imaging of nearby young disks have established that their structure is made of rings, gaps, spiral arms and other asymmetric substructures on spatial scales down to the resolution limit (> 5 au; e.g., ALMA Partnership et al. 2015; Benisty et al. 2015; Andrews et al. 2016, 2018; Isella et al. 2018).

These structures have emerged from both maps in scattered light in the optical and near infrared as well as for the dust thermal emission at longer sub-mm/mm wavelengths which probe grains in the disk midplane where planets are expected to form.

Most of these structures, especially the prominent rings and gaps, are thought to originate from gravitational perturbations by yet unseen planets in the act of forming. The modelling of the observed disk substructures provide a powerful tool to infer masses and orbital radii for the population of newborn planets which are still interacting with the parental disk (e.g., Zhang et al. 2018; Lodato et al. 2019). Given its very high sensitivity and angular resolution at long wavelengths, the Next Generation Very Large Array (ngVLA; Murphy et al. 2018) will have the right technical capabilities to unveil the signatures of the planet-disk interaction in the most efficient regions for the formation of planets, including terrestrial Earth-like planets, as demonstrated by previous ngVLA Community Studies (Ricci et al. 2018; Harter et al. 2020, ngVLA memo #33 and #57).

At the same time, these studies have focused on disk substructures in the thermal emission of dust, and no detailed studies on the ability of the ngVLA to detect and resolve structures in the molecular gas, which makes more than 90% of the mass of the disk, have been performed yet. Investigating the potential of the ngVLA to map structures due to the interaction with planets in the density and kinematics of the gas is particularly important to establish the link between the disk structures and the presence of planets, and rule out alternative physical mechanisms (e.g., magneto-hydrodynamic instabilities, condensation fronts, photoevaporation) that have been proposed in the literature to produce substructures in the dust.

In the last few years, ALMA high-res observations in molecular lines have detected substructures in the gas density as well as kinematic features in several young disks which are consistent with perturbations in the velocity field of the gas induced by embedded giant planets in the disk (Pinte et al. 2018, 2019, 2020). In most cases, these features are located inside the gaps observed in the dust emission, strongly favoring the hypothesis of planets carving those gaps. These perturbations to the molecular emission from a Keplerian disk model have specific morphologies that cannot be reproduced by any other physical mechanism studied so far, and are therefore considered to be the true smoking guns of planets embedded in disks (e.g., Pinte et al. 2022).

So far, ALMA has detected kinematic features in less than 10 disks and due to Jupiter-mass planets at > 50 au from the host star. Due to its very high angular and spectral resolutions and sensitivity, the ngVLA has the potential to detect planet signatures at lower separations from the star by imaging the molecular gas emission. In this study we present predictions of future ngVLA observations in the ^{12}CO ($J = 1 - 0$) line (rest frequency $\nu = 115.2712$ GHz), which falls within the high frequency end of ngVLA Band 6, for a disk with a velocity field perturbed by a Jupiter-mass planet at 20 au from the star.

Section 2 presents the methods used for this study, describing the disk physical models used to simulate the disk-planet interaction, the procedure used to obtain the model synthetic channel maps for the ^{12}CO ($J = 1 - 0$) emission line, and the method used to simulate the results of future ngVLA observations. Section 3 outlines the results of this investigation, whereas Section 4 presents the conclusion of this work.

2. Methods: from disk simulations to ngVLA observations

We describe here the method used to simulate observations with the ngVLA for the ^{12}CO ($J = 1 - 0$) line emission of disks with embedded Jupiter-mass planets.

2.1. Disk model

The models used for this investigation were obtained via 3D hydrodynamical planet–disk simulations using the grid-based hydrodynamics code `ATHENA++` in a spherical polar coordinate system (Stone et al. 2020). This code accounts for the dynamics of gas in a disk with one or more embedded planets. In particular, it can calculate the 3D velocity structure induced by the gravitational interaction between the disk gas and the planet, which is necessary to derive accurate predictions for the spatial variation of the gas emission at different frequencies across the line.

We refer to Rabago & Zhu (2021) for a detailed description of the physical structure of the disk models and method to extract 3D density, temperature and kinematics structures for a given model. In the models discussed here we considered a disk with an initial gas density which resembles the Minimum Mass Solar Nebula model (Hayashi 1981) around a Solar-mass young star. The disk has an outer radius of 60 au, and the temperature is similar to the one constrained observationally for the HD163296 disk (Isella et al. 2018), in which kinematic evidence for an embedded protoplanet has been obtained with ALMA (Pinte et al. 2018). In our simulations, the 3D velocity field of the gas is perturbed by the gravitational interaction with one planet embedded in the disk. All the results presented in this work are obtained with a Jupiter-mass planet orbiting at 20 au from the central star.

The gas density, temperature and velocity field obtained from the hydro simulations are used to derive synthetic channel maps for the ^{12}CO ($J = 1 - 0$) emission line via the ray-tracing module of `RADMC-3D` (Dullemond et al. 2012). In this work we show the results obtained for models with a disk inclination of 30 degrees, with the planet located at a position angle of −30 degrees around the star (position angle conventionally defined as the angle east of north), and at a distance of 140 pc. The abundance of CO, $n(\mathrm{CO})/n(\mathrm{H_2})$, used to produce the CO emission maps was 6×10^{-5}. The synthetic channel maps were obtained with a channel width of ≈ 0.52 km/s. Although channel maps with narrower channels were investigated and resulted into better defined kinematic perturbations in the synthetic images, channel maps with channel width of 0.52 km/s were found to be better suited for the detection of the planet-induced kinematic signatures in reasonable observational times with the ngVLA for the model discussed here.

2.2. Simulations of the ngVLA observations

The synthetic maps obtained according to the method outlined in Section 2.1 were converted into predictions for future observations with the ngVLA using the CASA software package (McMullin et al. 2007). We adopted the same procedure as in Ricci et al. (2018), in which the ngVLA simulations are performed using the `SIMOBSERVE` task to generate the visibility dataset in the (u, v) Fourier space, and using `setnoise` to add the noise by corrupting the visibilities. The only difference with that study is that in this work this procedure was extended to the synthetic 3D datacube containing the individual channel maps, rather than to a single map representing the dust continuum emission.

For the ngVLA simulations we considered the ngVLA Rev D array configuration with antennas distributed across North America and Mexico[1]. The Rev D configuration includes 214 antennas of 18 meter diameter, with minimum and maximum baselines of $\approx$ 39 and 1068 km, respectively (ngVLA memo #92). We instead did not include the 30 additional antennas distributed to baselines up to 9000 km, as the signal from the sources considered here would be very faint for these very long baselines. Before imaging of the emission line, we performed a subtraction of the continuum emission in the (u, v) plane using the `uvcontsub` CASA task. We then imaged the visibilities using the `CLEAN` algorithm (`tclean` in CASA) with Briggs weighting, and adjusted the robust parameter to give a reasonable synthesized beam and noise performance. In particular, the ngVLA images were computed with a Briggs weighting with robust parameter $R = -1$. We also employed a multiscale clean approach to better recover compact emission at both high brightness and large diffuse structures in the model, and we tested outer tapering of the interferometric visibilities to optimize the detectability and signal-to-noise ratio of the kink structures discussed in the previous Section, at the expense of angular resolution. The disk center was located at a declination of +24.0 degrees for the ngVLA simulations.

3. Results

Figure 1 shows the synthetic channel maps for the ^{12}CO ($J = 1 - 0$) line emission derived from our model. In each channel, the line emission is concentrated along an isovelocity curve, i.e. the region where the projected velocity of the emitting surface is constant. Because of the Keplerian rotation of the disk and correspondent Doppler shift, this isovelocity curve follows a typical "butterfly" pattern (Horne & Marsh 1986).

A perfectly Keplerian disk results in smooth iso-velocity contours and velocity channel maps described by the butterfly pattern. However, our disk is gravitationally perturbed by a Jupiter-mass planet, and this results into two effects that are visible in Figure 1. The first and more evident effect is that the wings of the butterfly are "broken" at the location of the gap opened in the disk by the Jupiter-mass planet[2].

The second effect is due to more local perturbations induced by the planet on the velocity of the gas in the disk. These velocity perturbations will change the projected velocity of the emitting gas and shift the emission into an adjacent channel. As a consequence, in a given channel, these velocity perturbations result in "kinks" which modify the butterfly pattern characteristic of Keplerian rotation. In some channels these features can reconnect the inner and outer sides of the butterfly wings, which in other channels are broken by the gap opened by the planet. Since this is a local effect, these kink structures are seen only in the channels in which the gas emission "sweeps through" the location of the planet on the map. In Figure 1 these are best visible in channels -2.84 and -2.32 km/s, on the top emitting layer. Note that these features are not visible in either the bottom emitting layer in those channels or in the top and bottom emitting

[1]The configuration file can be downloaded at `https://ngvla.nrao.edu/page/tools`

[2]Note that the only channels in which this feature is not visible are the highest velocity channels shown in Figure 1, as at these velocities only the inner disk regions at stellocentric radii $r < r_{\rm gap}$ contribute to the emission.

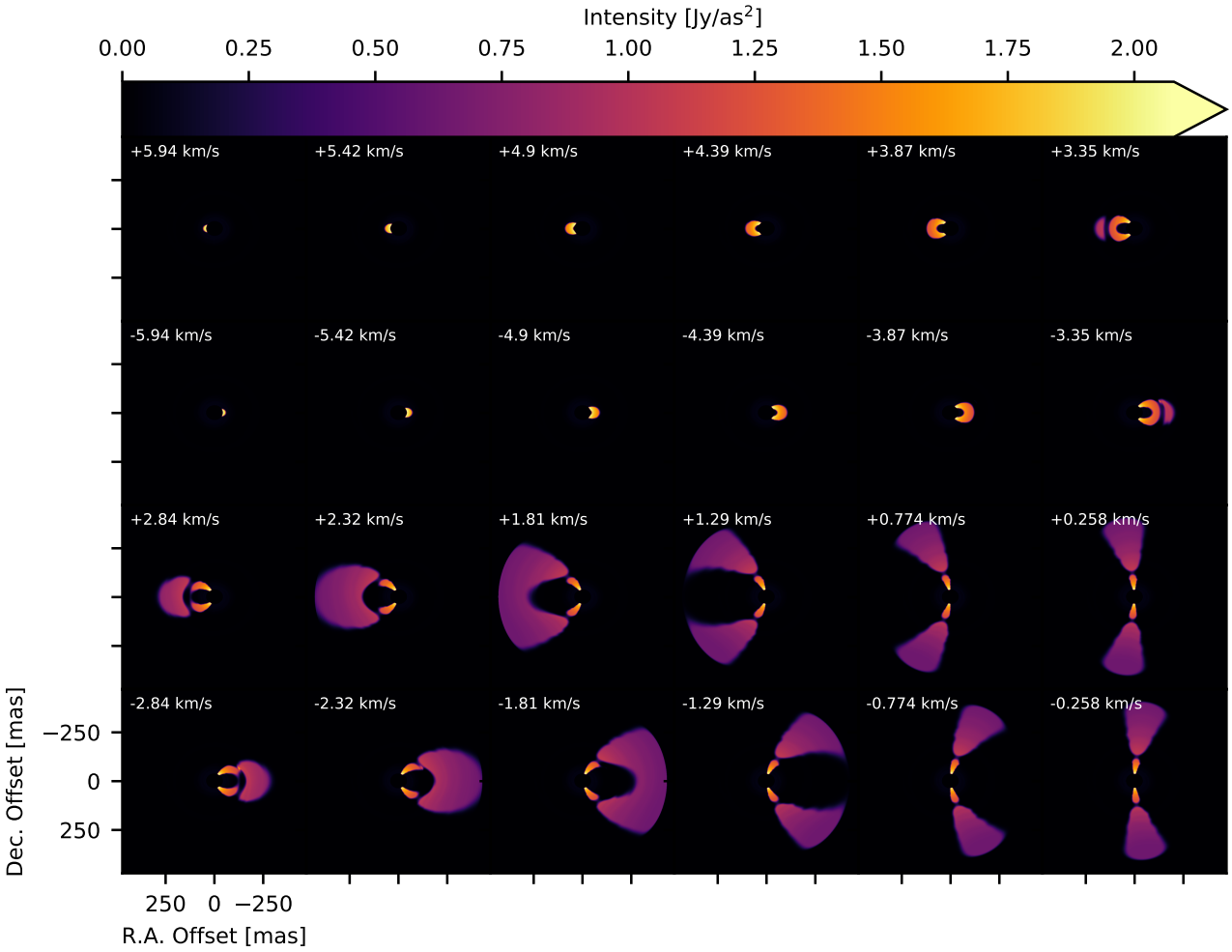

Figure 1. Model synthetic channel maps for the ^{12}CO ($J = 1-0$) line emission for the disk+planet system considered in this study. The central channel velocity relative to the rest frame velocity of the system is shown on the top side of each panel.

layers in the Doppler-symmetric channels at velocities of +2.84 and +2.32 km/s, and directly trace the location of the planet inside the gap.

Figure 2 shows the results of the ngVLA simulated observations. At the distance of 140 pc, the spatial resolution of these observations is $\approx$ 1 au. In this figure we show only the channels where the CO emission sweeps through the location of the planet (bottom row), together with the Doppler-symmetric channels (top row) to highlight the asymmetric nature of the kink structure. This channel map shows that the ngVLA has the potential to detect the resolve the kinematic kink structure induced by a Jupiter-mass planet at an orbital radius of 20 au.

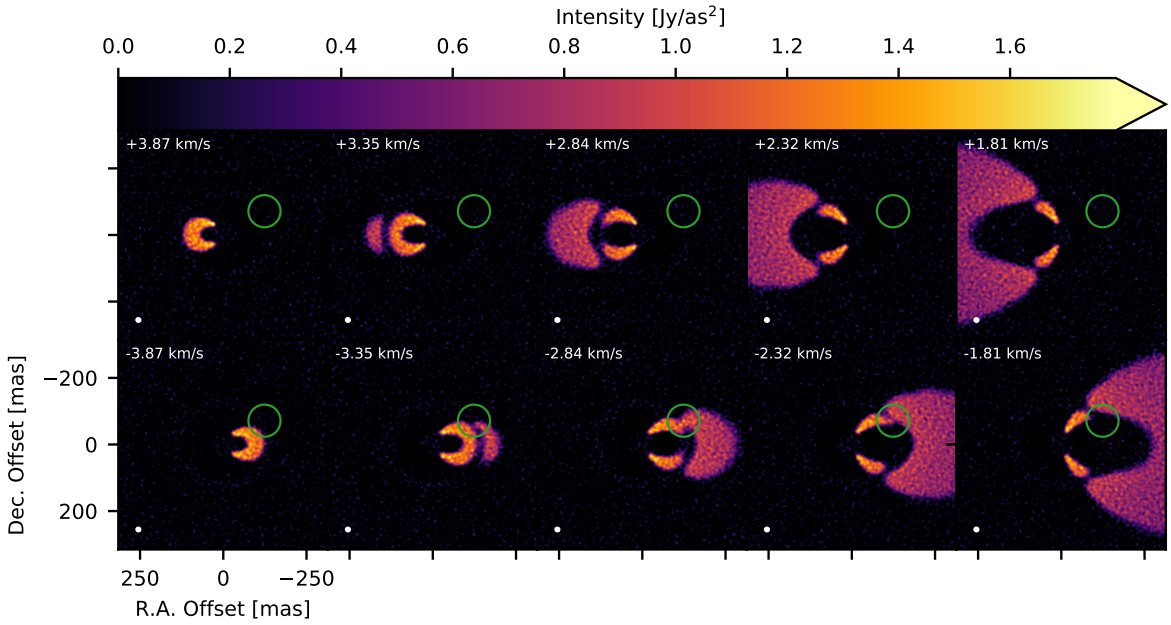

Figure 2. ngVLA channel maps for the ^{12}CO ($J = 1 - 0$) emission line for the disk model presented in this study. The bottom row shows only the channels where the CO emission region sweeps through the location of the planet. The top row shows the Doppler-symmetric channels to highlight the asymmetry in the emission due to the velocity perturbations induced by the planet. In each panel, the white ellipse on the bottom left corner represents the synthesized beam, which has sizes of 9.6 mas × 8.9 mas with a position angle of 77°. The green circle indicates the location of the planet. The 1σ rms noise on each channel map is 10 μJy/beam.

At the same time, according to the current ngVLA specifications[3], a 1σ rms noise of 10 μJy/beam within a 0.5 km/s wide channel within ngVLA Band 6, as in Figure 2, can be obtained only with a long integration time of $\approx$ 150 hr.

The impact of the rms noise on the observability of the gap and kink structures induced by the Jupiter-mass planet is investigated in Figure 3. This figure shows that these structures should be observable even with a rms noise of $\approx$ 20 μJy/beam, achievable in $\approx$ 40 hr of integration time. ngVLA observations with shorter integration times would be able to detect the gap opened by the planet and possibly also find evidence for the local enhancement of the gas emission in the regions of the gap closest to the planet, but follow-up observations with longer integration times ($>$ 10 hr) would be likely necessary to resolve the kink structure and characterize the planet properties via a detailed modeling of the disk gas emission.

[3]See https://ngvla.nrao.edu/page/performance

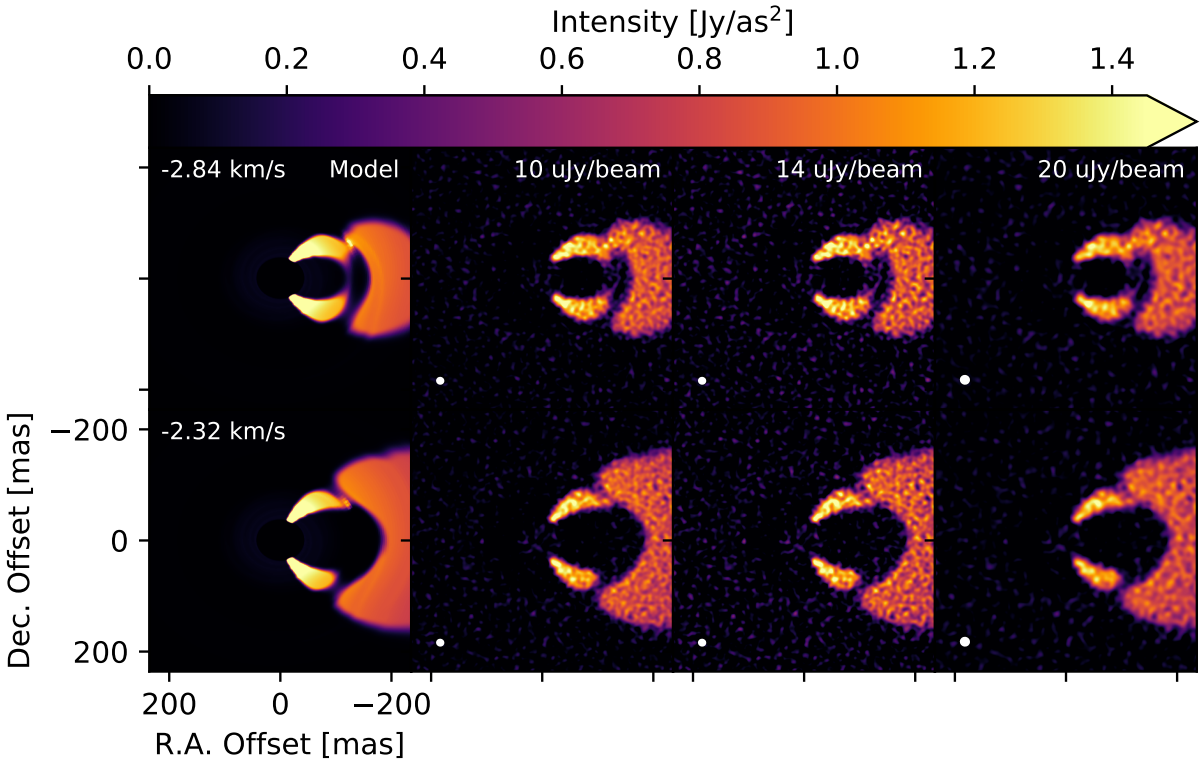

Figure 3. ^{12}CO ($J = 1-0$) emission from the channels with $v = -2.84$ km/s and $v = -2.32$ km/s to highlight the kink structure produced by the planet. From left to right: model image; ngVLA simulated observations with 1σ rms noise of 10 μJy/beam and beam size of $\approx$ 9.3 mas; ngVLA simulated observations with 1σ rms noise of 14 μJy/beam and beam size of $\approx$ 9.3 mas; ngVLA simulated observations with 1σ rms noise of 20 μJy/beam and beam size of $\approx$ 13.0 mas. Note that different outer taper values of the interferometric visibilities were used to obtain the beam sizes presented here.

4. Conclusions

The ngVLA will transform the fields of planet formation and protoplanetary disks, allowing for imaging of the disk physical structure at very high resolution and sensitivity in nearby star forming regions.

In this study we tested the imaging capabilities of the ngVLA to detect and resolve the substructures expected in the channel maps of the ^{12}CO ($J = 1 - 0$) emission line as produced by a Jupiter-mass planet orbiting a young Solar-mass star at a separation of 20 au.

We show that these kinematic features can be detected and spatially resolved with a few tens of hours of observation time with the ngVLA. As this may be the only viable method to find evidence for young protoplanets that are deeply embedded in their parental disk, these results further strengthen the case for the ngVLA for the investigation of the formation and early evolution of planetary systems.

This work presents the results of one specific disk+planet model. Further details on this model as well as the predictions for future ngVLA observations over a broader

region of the parameter space of the models will be provided in a future paper (Ricci et al. in prep.).

Acknowledgments. This work was supported by the ngVLA Community Studies program, coordinated by the National Radio Astronomy Observatory, which is a facility of the National Science Foundation operated under cooperative agreement by Associated Universities, Inc.

References

ALMA Partnership et al. 2015, ApJ, 808, 3
Andrews, S. 2020, ARA&A 58, 483
Andrews, S., Huang, J., Perez, L., et al. 2018, ApJ 869, 41
Andrews, S., Wilner, D., Zhu, Z. et al. 2016, ApJ, 820, 40
Benisty, M., Juhasz, A., Boccaletti, A., et al. 2015, A&A 578, 6
Burrill, B., Ricci, L., Harter, S. K. et al. 2022, ApJ 928, 40
Dullemond, C. P., Juhasz, A., Pohl, A. et al. 2012, ascl:1202.015
Harter, S. K., Ricci, L., Zhang, S., Zhu, Z. 2020, ApJ 905, 24
Hayashi, C. 1981, PThPS 70, 35
Horne K. & Marsh T. R., 1986 MNRAS, 218, 761
Isella, A., Huang, J., Andrews, S. et al. 2018, ApJ, 869, 49
Lodato, G., Dipierro, G., Ragusa, E., et al. 2019, MNRAS 486, 453
McMullin, J. P., Waters, B., Schiebel, D., Young, W., & Golap, K. 2007, in ASP Conf. Ser. 376, Astronomical Data Analysis Software and Systems XVI (San Francisco, CA: ASP), 127
Murphy, E. J., Bolatto, A., Chatterjee, S. et al. 2018, Science with a Next Generation Very Large Array, ASP Conference Series, Vol. 517. ASP Monograph 7. Edited by Eric Murphy., p.3
Pinte, C., Teague, R., Flaherty, K. et al. 2022, arXiv:2203.09528, Chapter for Protostars & Planets VII
Pinte, C., Price, D. J., Menard, F., et al. 2020, ApJ 890, 9
Pinte, C., van der Plas, G., Menard, F., et al. 2019, Nature Astronomy 3, 1109
Pinte, C., Price, D. J., Menard, F., et al. 2018, ApJ 860, 13
Rabago, I., & Zhu, Z. 2021, MNRAS 502, 5325
Ricci, L., Liu, S.-F., Isella, Andrea; Li, H. 2018, ApJ 853, 110
Sanchis, E., Picogna, G., Ercolano, B., Testi, L., Rosotti, G. 2020, MNRAS 492, 3440
Stone, J. M., Tomida, K., White, C. J., Felker, K. G. 2020, ApJS 249, 4
Zhang, S., Zhu, Z., Huang, J., Guzman, V. et al. 2018, ApJ 869, 47